

# Geometric Reinforcement Learning: The Case of Cartesian Space Orientation

NASEEM ALHOUSANI<sup>1</sup>, MATTEO SAVERIANO<sup>2</sup>, *Member, IEEE*, IBRAHIM SEVINC<sup>3</sup>, TALHA ABDULKUDDUS<sup>3</sup>, HATICE KOSE<sup>1</sup>, *Member, IEEE*, and FARES J. ABU-DAKKA<sup>4</sup>, *Member, IEEE*

**Abstract**—Reinforcement learning (RL) enables an agent to learn by trial and error while interacting with a dynamic environment. Traditionally, RL is used to learn and predict Euclidean robotic manipulation skills like positions, velocities, and forces. However, in robotics, it is common to have non-Euclidean data like orientation or stiffness, and neglecting their geometric nature can adversely affect learning performance and accuracy. In this paper, we propose a novel framework for RL by using Riemannian geometry, and show how it can be applied to learn manipulation skills with a specific geometric structure (e.g., robot's orientation in the task space). The proposed framework is suitable for any policy representation and is independent of the algorithm choice. Specifically, we propose to apply policy parameterization and learning on the tangent space, then map the learned actions back to the appropriate manifold (e.g., the  $S^3$  manifold for orientation). Therefore, we introduce a geometrically grounded pre- and post-processing step into the typical RL pipeline, which opens the door to all algorithms designed for Euclidean space to learn from non-Euclidean data without changes. Experimental results, obtained both in simulation and on a real robot, support our hypothesis that learning on the tangent space is more accurate and converges to a better solution than approximating non-Euclidean data.

**Index Terms**—Learning on manifolds, policy optimization, policy search, geometric reinforcement learning.

## I. INTRODUCTION

THE impressive success of robots in the field of automation comes at the cost of strong limitations on the robot's workspace and the performed tasks. Indeed, industrial manipulators usually operate in a structured and static environment and are pre-programmed to perform repetitive tasks. Artificial intelligence has the potential to relieve these limitations and to allow autonomous robots to perform tasks in a dynamic environment [1] while constantly adapting to changes in their surroundings [2]. Reinforcement Learning (RL) is a key part in making robots autonomous as a robot can learn by interacting with its environment, guided by a

scalar that represents the reward of its taken action. Nowadays, the practical applications of RL have become many and span various fields, from medical and economic applications to the fields of networking, communication, and natural language processing [3]. The introduction of deep learning techniques in RL allows for high-dimensional state spaces to be represented by low-dimensional features through the use of neural networks. This made applying RL to robotics a more viable task, as the compact feature representation along with powerful generalization lends itself well to the continuous state-space nature of robotic environments [4].

The application of RL in robotics involves great challenges such as the long training time [5] or the design of the goal through the reward function, as it usually needs to be known in advance [6]. This reward challenge has been addressed in different ways, including Learning from Demonstration (LfD) [7], inverse RL [8], or a combination of the two [9]. An important issue is the safety of the robot and its environment [10], as it requires high accuracy in terms of both state representation and learned policy.

An alternative method for policy improvement is through Black Box Optimization (BBO). BBO algorithms are general methods that optimize a given objective function, yet make no assumptions about said function or the defined search space [11]. One notable BBO algorithm is Covariance Matrix Adaptation Evolution Strategy (CMA-ES) [12]. It is a derivative-free optimization algorithm that also implements an evolution strategy, using mechanisms like mutation, recombination, and selection. These mechanisms help filter out poor solutions and produce new ones that better optimize the objective function.

Non-Euclidean data (e.g., orientation, stiffness, or manipulability) are important in the field of robotics as they are widely used during learning and implementation processes [13]. Such data have special properties that do not allow for Euclidean calculus and algebra to be used. Despite this, they are usually treated as Euclidean data which demands pre- or post-processing (e.g., normalizing orientation data) to conform to their non-Euclidean nature. This process involves an approximation, and with repetition, the approximation errors will accumulate until it reaches a level that affects the learning process in terms of both accuracy and speed to reach the desired results. This issue was noticed early in the field of statistical learning [14], as determining the center of a non-Euclidean geometric data set using normalization leads to an error in determining the mean.

In this paper, we propose a novel RL framework exploiting

<sup>1</sup>Faculty of Computer and Informatics, Istanbul Technical University, Maslak, 34467 Sarıyer/Istanbul, Turkey (e-mail: nalhousani@itu.edu.tr, hatice.kose@itu.edu.tr)

<sup>2</sup>Department of Industrial Engineering (DII), University of Trento, Trento, 38123, Italy (e-mail: matteo.saveriano@unitn.it)

<sup>3</sup>ILITRON Enerji ve Bilgi Teknolojileri A.Ş., Sultan Selim Mahallesi, Akyol Sanayi Sitesi Çıkmaşı No:10/1 Kağıthane İstanbul (e-mail: ibrahim-sevinc@ilitron.com, talha.abdulkuddus@ilitron.com)

<sup>4</sup>Intelligent Robotics Group, Department of Electrical Engineering and Automation (EEA), Aalto University, Espoo, Finland (e-mail: fares.abu-dakka@aalto.fi)

This work has been partially supported by The Scientific and Technological Research Council of Turkey (TÜBİTAK) under Grant 3201141, and by CHIST-ERA project IPALM (Academy of Finland decision 326304).

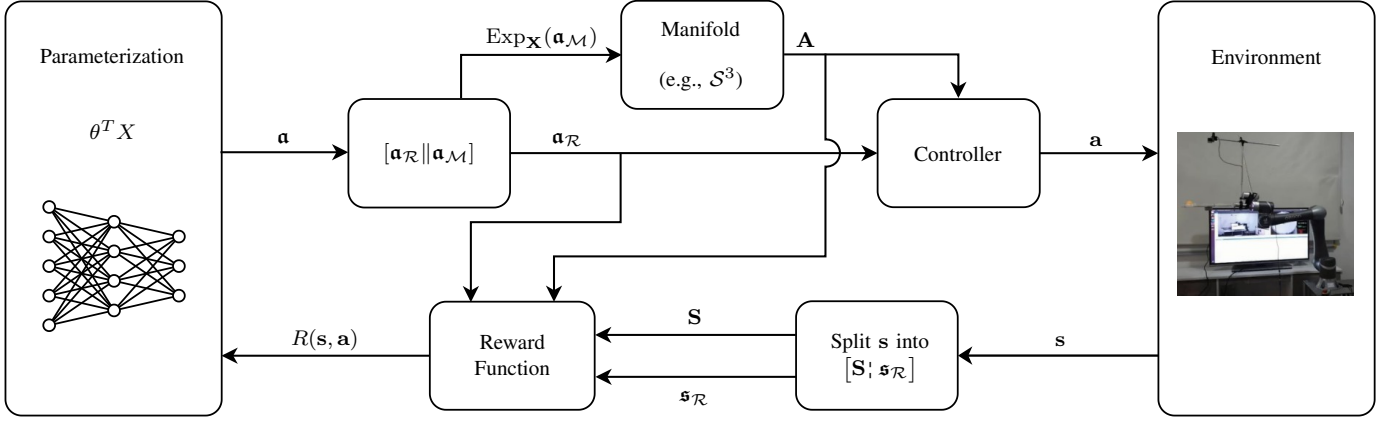


Fig. 1. Overview of the proposed framework applying reinforcement learning on the bounded tangent space (e.g.,  $\mathcal{R}^3$ ). Starting with the result of parameterization, it is mapped to the (e.g.,  $\mathcal{S}^3$ ) manifold, and the resultant manifold data is passed to controller to execute the action. The current state data is then collected, split into Euclidean and manifold parts, and sent to the reward function to evaluate the quality of the executed action. This evaluation is delivered back to the RL algorithm.

the geometric structure of the data using Riemannian geometry, to apply policy parameterization on a tangent space, then mapping the result to its corresponding manifold. As a case study, we apply the proposed approach to learn and predict orientation data represented as unit quaternions. Moreover, our framework is independent of the choice of the RL algorithm, whether it is model-free [15], [16] or model-based [17], [18]. It is also valid for deep reinforcement learning algorithms (e.g., [19]–[22]), regardless of whether it is deterministic or probabilistic. Furthermore, our proposed approach can be applied to BBO algorithms like CMA-ES [12], which then can be used as a policy improvement method like in [11]. An overview of the proposed approach is shown in Fig. 1.

## II. RELATED WORK

In general, typical RL algorithms using a Gaussian distribution (e.g., [15]–[22]) are not accurate when learning non-Euclidean data, as that data sits in curvature space and not vector space. RL algorithms must provide non-Euclidean data special treatment to avoid approximation and to respect the unique properties of that data. This has been approached in different ways.

The Riemannian manifold, Riemannian metric, and tangent space concepts have been utilized in creating geometrical tools for statistics as in [14], which have been used in different research works. Abu-Dakka *et al.* [23] leveraged Riemannian geometry in the context of learning robotic manipulation skills (e.g., stiffness) using a kernelized treatment in the tangent space. Zeestraten *et al.* [24] proposed a framework for imitation learning on Riemannian manifolds and built on it [25] to derive a Linear Quadratic Regulator (LQR) tracking controller on  $\mathcal{S}^3$ . Instead of only using Cartesian coordinate systems, the work in [26] exploits a dictionary of coordinate systems for encoding the observed behaviors, then treats the problem as a general optimal control problem using an iterative LQR (iLQR). Similar ideas were applied in Probabilistic Movement Primitives (ProMPs) to learn from demonstration [27]. Huang *et al.* [28] proposed adapting learned orientation trajectories to pass through via-points or

end-points while also considering the angular velocity. Work done in [29] utilizes a variational autoencoder (VAE) to learn geodesics on Riemannian manifolds using LfD, which generates end-effector pose trajectories able to dynamically avoid obstacles present in the environment. In the context of image segmentation, authors in [30] proposed a method for 3D image reconstruction by adapting the original CMA-ES to Riemannian manifolds and applying optimization on the tangent space. Parameterization on the tangent space is used in computer vision for regressing rotations using deep learning [31].

The extension of optimization algorithms to Riemannian manifolds has also been investigated. In [32], Bayesian Optimization (BO) related algorithms were used to optimize policy parameters. Authors proposed geometry-aware kernels which allow proper measuring of the similarity between Riemannian manifold parameters using the Gaussian process (GP). Recently, authors of [33] implemented the geometry-aware Riemannian Matérn kernels in the context of robotics.

Although there are many existing works in the field of LfD and supervised learning, Riemannian geometry has not been exploited in RL. A recent work, Bingham Policy Parameterization (BPP) [34], uses the Bingham distribution as an alternative to the Gaussian distribution for learning orientation policies. This choice was motivated by the argument that unit quaternions can be directly sampled from the Bingham distribution unlike the Gaussian distribution, where one must use normalization. Nevertheless, authors in [34] reported that as their implementation uses several neural networks, instability in the learning process could occur if erroneous data is sampled from them. We experimentally compare the performance of our approach and BPP in Sec. V-A1.

Inspired by supervised approaches for manifold learning, we extend RL approaches to Riemannian manifolds by parameterizing the policy on the tangent space. Due to the nature of the space, which can be locally considered as a Euclidean space, all that is required is mapping the action resulting from the tangent space policy to the appropriate manifold, measuring the quality of the action by implementing it in

a robot, and harvesting the reward. Thus, all policy search algorithms can be straightforwardly adapted to manifold data, yielding a higher-quality policy.

### III. BACKGROUND

#### A. Reinforcement Learning

The general formulation of a typical RL problem is about an agent at time  $t$  in state  $s_t$  selecting an action  $a_t$  according to a stochastic policy

$$\pi_{\theta}(\mathbf{a}, \mathbf{s}) = \Pr(\mathbf{a} = \mathbf{a}_t \mid \mathbf{s} = \mathbf{s}_t), \quad (1)$$

where  $\theta \in \mathcal{R}^n$  are the parameters of the policy and  $\pi$  is the probability distribution of sampling action  $a_t$  in state  $s_t$  at time  $t$ . Performing action  $a_t$  changes the world state to  $s_{t+1}$  and the agent receives a reward  $r_{t+1}$ , associated with the transition  $T(s_t, a_t, s_{t+1})$ . The agent's objective is to maximize the expected return of the policy [35], i.e.,

$$\max_{\theta} \mathbb{E}_{\pi_{\theta}} [R(\mathbf{s}, \mathbf{a})] = \max_{\theta} \mathbb{E}_{\pi_{\theta}} \left[ \sum_t r(s_t, \mathbf{a}_t) \right]. \quad (2)$$

In this paper, we have used different RL algorithms and a BBO algorithm for policy search, to show the versatility of our proposed approach. The used algorithms are briefly reviewed as follows.

1) *PoWER*: Policy learning by Weighting Exploration with the Returns (PoWER) [36] is an RL policy search algorithm inspired by expectation maximization in supervised learning algorithms. It is designed for finite horizons with episodic restarts and uses an average return as a weight instead of a gradient.

2) *SAC*: Soft Actor-Critic (SAC) [21] is an instance of entropy-regularized deep RL, which aims to maximize the policy's return while also maximizing entropy. An entropy coefficient is used to control the importance of entropy and is adjusted during training.

3) *PPO*: Proximal Policy Optimization (PPO) [22] is a deep RL policy gradient optimization algorithm that clips policy gradient updates to a narrow interval, ensuring the new policy is not too far from the existing one.

4) *CMA-ES*: CMA-ES [12] is a derivative-free method for non-linear or non-convex BBO problems in the continuous domain. Instead of using gradient information, CMA-ES makes use of evolutionary computation and an evolution strategy to solve the optimization problem.

#### B. Riemannian manifold

A Riemannian manifold  $\mathcal{M}$  is an  $n$ -dimensional smooth differentiable topological space equipped with a Riemannian metric, that locally resembles the Euclidean space  $\mathcal{R}^n$ . The locally Euclidean tangent space  $\mathcal{T}_{\mathbf{X}}\mathcal{M}$  can be constructed around any point  $\mathbf{X} \in \mathcal{M}$ . The Riemannian metric can be used to generalize the notion of the straight line between two points in Euclidean space by defining the shortest curve between two points in a manifold, which is denoted as a geodesic.

In order to go back and forth between a manifold  $\mathcal{M}$  and a tangent space  $\mathcal{T}_{\mathbf{X}}\mathcal{M}$ , we require two distance-preserving

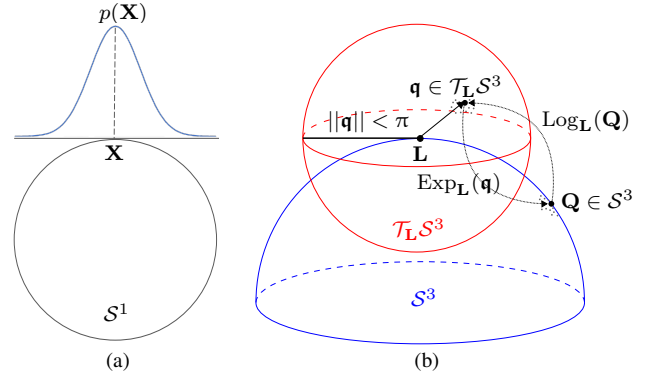


Fig. 2. (a)  $S^1$  manifold, sampling from Gaussian distribution, where the mean is on  $S^1$  but the drawn samples are not, unless the drawn sample is the mean itself. (b) A red sphere representing the bounded tangent space of the lie algebra  $\mathcal{T}_{\mathbf{L}}S^3$ . The blue hemisphere surface excluding the equator represents the corresponding space on the  $S^3$  manifold. The mapping functions between the two spaces is shown.

mapping functions (operators). These operators are (i) the exponential map  $\text{Exp}_{\mathbf{X}} : \mathcal{T}_{\mathbf{X}}\mathcal{M} \rightarrow \mathcal{M}$ , and its inverse (ii) the logarithmic map  $\text{Log}_{\mathbf{X}} : \mathcal{M} \rightarrow \mathcal{T}_{\mathbf{X}}\mathcal{M}$ . It is possible to show that exponential and logarithmic maps are (locally) bijective, which makes it possible to do the calculations about the non-Euclidean manifold space on the tangent space and project back the results.

### IV. POLICY PARAMETERIZATION ON TANGENT SPACE

Gaussian policy parameterization has a limitation when it comes to representing non-Euclidean data like orientation, as the distribution parameters (both mean and variance) do not always obey the nature of the manifold's curvature space. The problem with sampling non-Euclidean from a Gaussian distribution is illustrated in Fig. 2 (a) for the  $S^1$  manifold, i.e., the circumference of the unit circle. Picking a point on the manifold to be the mean of the normal distribution, samples can still be drawn from outside the manifold as illustrated in the figure. Normalization of the sample can map it back to the unit circle manifold at the cost of accuracy. The same argument is applicable to other manifolds like  $S^3$  embedded in  $\mathcal{R}^4$ , as in Fig. 2 (b). To this point, using Gaussian policy parameterization like SAC [21] or PPO [22] on quaternion data will require normalizing the predicted profiles. This kind of post-processing is an approximation that could affect learning accuracy.

It is beneficial to have a framework allowing for well-established and stable learning algorithms on Euclidean space to be transferred to other geometrical spaces with relative ease and reasonable computational costs. This enables all the achievements and progress that have been made on Euclidean space to be directly applicable to non-Euclidean spaces. We propose a general framework that is independent of the choice of both the parameterization scheme and the optimization algorithm.

If the state  $\mathbf{s}$  involves both Euclidean and manifold data, like a Cartesian pose where  $\mathbf{s} \in S^3 \times \mathcal{R}^3$ , then we split  $\mathbf{s}$  into a manifold part  $\mathbf{S}$  and a Euclidean part  $\mathbf{s}_{\mathcal{R}}$ , i.e.,  $\mathbf{s} = [\mathbf{S}; \mathbf{s}_{\mathcal{R}}]$ . Similarly, we split the action as  $\mathbf{a} = [\mathbf{A}; \mathbf{a}_{\mathcal{R}}]$ . The splits allow

**Algorithm 1** Geometric reinforcement learning with policy parameterization on tangent space

**Input:** initial state  $\mathbf{s}_0$ , initial parameters  $\boldsymbol{\theta}$ , and the RL algorithm  $\alpha$ .

```

1: while !stop_condition( $\alpha$ ) do
2:    $\pi_{\boldsymbol{\theta}}(\mathbf{a}, \mathbf{s}) \leftarrow \text{get\_policy}(\boldsymbol{\theta}, \alpha)$   $\triangleright$  eq. (4)
3:    $R(\mathbf{s}, \mathbf{a}) \leftarrow 0$   $\triangleright$  cumulative reward
4:   for  $t = 0, \dots, T - 1$  do
5:      $\mathbf{s}_t = [\mathbf{S}_t'; \mathbf{s}_{\mathcal{R},t}]$ 
6:      $\mathbf{s}_{\mathcal{M},t} \leftarrow \text{Log}_{\mathbf{X}}(\mathbf{S}_t)$ 
7:      $\mathbf{s}_t \leftarrow [\mathbf{s}_{\mathcal{M},t} \| \mathbf{s}_{\mathcal{R},t}]$   $\triangleright$  state concatenation (3)
8:      $\mathbf{a}_t \leftarrow \pi_{\boldsymbol{\theta}}(\mathbf{a}, \mathbf{s}_t)$   $\triangleright$  tangent space action (5)
9:      $\mathbf{a}_t = [\mathbf{a}_{\mathcal{M},t} \| \mathbf{a}_{\mathcal{R},t}]$   $\triangleright$  action concatenation (3)
10:     $\mathbf{a}_t \leftarrow [\text{Exp}_{\mathbf{X}}(\mathbf{a}_{\mathcal{M},t}); \mathbf{a}_{\mathcal{R},t}]$   $\triangleright$  manifold action (6)
11:     $\mathbf{s}_{t+1} \leftarrow \text{execute\_on\_robot}(\mathbf{a}_t)$ 
12:     $R(\mathbf{s}, \mathbf{a}) \leftarrow R(\mathbf{s}, \mathbf{a}) + r(\mathbf{s}_t, \mathbf{a}_t)$ 
13:   end for
14:   return  $R(\mathbf{s}, \mathbf{a})$ 
15:    $\boldsymbol{\theta} \leftarrow \text{improve\_policy}(\boldsymbol{\theta}, R(\mathbf{s}, \mathbf{a}), \alpha)$ 
16: end while

```

projecting the state  $\mathbf{s}$  and the action  $\mathbf{a}$  in the tangent space of the composite manifold as

$$\begin{aligned}\mathbf{s} &= [\mathbf{s}_{\mathcal{M}} \| \mathbf{s}_{\mathcal{R}}] = [\text{Log}_{\mathbf{X}}(\mathbf{S}) \| \mathbf{s}_{\mathcal{R}}], \\ \mathbf{a} &= [\mathbf{a}_{\mathcal{M}} \| \mathbf{a}_{\mathcal{R}}] = [\text{Log}_{\mathbf{X}}(\mathbf{A}) \| \mathbf{a}_{\mathcal{R}}],\end{aligned}\quad (3)$$

where  $[\cdot \| \cdot]$  is a concatenation operator. Intuitively, the projection on the tangent space allows us to “stack” manifold and Euclidean parts into a unique vector. The policy  $\pi_{\boldsymbol{\theta}}$  is computed using  $\mathbf{s}$  and  $\mathbf{a}$  in (3) as

$$\begin{aligned}\pi_{\boldsymbol{\theta}}(\mathbf{a}, \mathbf{s}) &= [\pi_{\boldsymbol{\theta}_{\mathcal{M}}}(\mathbf{a}_{\mathcal{M}}, \mathbf{s}_{\mathcal{M}}) \| \pi_{\boldsymbol{\theta}_{\mathcal{R}}}(\mathbf{a}_{\mathcal{R}}, \mathbf{s}_{\mathcal{R}})] \\ &= [\pi_{\boldsymbol{\theta}_{\mathcal{M}}}(\text{Log}_{\mathbf{X}}(\mathbf{A}), \text{Log}_{\mathbf{X}}(\mathbf{S})) \| \pi_{\boldsymbol{\theta}_{\mathcal{R}}}(\mathbf{a}_{\mathcal{R}}, \mathbf{s}_{\mathcal{R}})],\end{aligned}\quad (4)$$

where  $\boldsymbol{\theta} = [\boldsymbol{\theta}_{\mathcal{M}} \| \boldsymbol{\theta}_{\mathcal{R}}]$  is the concatenation of parameters for the manifold and Euclidean part, respectively.

At each time  $t$ , an action  $\mathbf{a}_t = [\mathbf{a}_{\mathcal{M},t} \| \mathbf{a}_{\mathcal{R},t}]$  is drawn from the policy (4), projected on the composite manifold via the exponential map, and sent to the agent. In formulas

$$\mathbf{a}_t \sim [\pi_{\boldsymbol{\theta}_{\mathcal{M}}}(\mathbf{a}_{\mathcal{M}}, \mathbf{s}_{\mathcal{M},t}) \| \pi_{\boldsymbol{\theta}_{\mathcal{R}}}(\mathbf{a}_{\mathcal{R}}, \mathbf{s}_{\mathcal{R},t})], \quad (5)$$

$$\mathbf{a}_t = \text{Exp}_{\mathbf{X}}(\mathbf{a}_t) = [\text{Exp}_{\mathbf{X}}(\mathbf{a}_{\mathcal{M},t}); \mathbf{a}_{\mathcal{R},t}]. \quad (6)$$

The agent performs the resulting manifold action  $\mathbf{a}_t$  on the environment. This causes the state to transition from  $\mathbf{s}_t$  to  $\mathbf{s}_{t+1}$ . The expected quality of the policy is captured by the expected return

$$\begin{aligned}\mathbb{E}_{\pi_{\boldsymbol{\theta}}} \left[ \sum_t r(\mathbf{s}_t, \mathbf{a}_t) \right] &= \\ \mathbb{E}_{\pi_{\boldsymbol{\theta}}} \left[ \sum_t r([\mathbf{S}_t'; \mathbf{s}_{\mathcal{R},t}], [\mathbf{A}_t'; \mathbf{a}_{\mathcal{R},t}]) \right].\end{aligned}\quad (7)$$

As shown in Algorithm 1, the initial state and RL algorithm are used as input. In line 2, the RL algorithm generates a policy structure with the current parameters  $\boldsymbol{\theta}$ . The policy is used in the next rollout (lines 4–13) to control the robot. In particular, given the state projected on the tangent space

of the composite manifold (lines 5–7), we sample an action from the given policy (line 8), project it to the composite manifold (lines 9–10), and send it to the robot (line 11). After one rollout is finished, the quality of the policy is measured using the rollout reward which is passed to the RL algorithm (line 14) to proceed with learning (line 15). This procedure is repeated until the stopping criteria, depending on the used RL algorithm, is met (line 1).

*Case Study:* Recently, the topic of learning using Riemannian geometry tools has become the focus of researchers in the field of robot learning [23], [37]–[39]. An example of non-Euclidean data is the end-effector orientation, a part of a robot’s operational space along with its Cartesian position. It is common to apply learning in this space since it allows for kinematic redundancy and the ability to transfer a learned policy from one robot to another robot with different anatomy [13].

Orientations are commonly represented using rotation matrices, Euler angles, or unit quaternions. Euler angles are a minimal orientation representation (requiring only 3 parameters), but they suffer from the singularity problem [40]. Unit quaternions hold an advantage over rotation matrices due to requiring fewer parameters (4 instead of 9) and are therefore commonly used to represent rotation in robotic applications. The unit quaternion representation belongs to the 3-sphere manifold  $\mathcal{S}^3$  [40]. Consequently, applying current reinforcement learning algorithms to learn an orientation policy is not straightforward as it normally involves approximations to respect the manifold structure.

In this paper, we focus on orientation learning represented by unit quaternions as a case study. A quaternion  $\mathbf{Q}$  is a tuple  $(v, \mathbf{u})$  consisting of a scalar  $v$  and a three-dimensional vector  $\mathbf{u} = (x, y, z)$ . Unit quaternions are quaternions with unity norm and are elements of  $\mathcal{S}^3$ . The hypersphere  $\mathcal{S}^3$  double-covers  $\mathcal{SO}(3)$ , therefore for every rotation in  $\mathcal{SO}(3)$  there are two quaternions that represent it ( $\mathbf{Q}$  and  $-\mathbf{Q}$ ). In this study, actions are unit quaternions and elements of  $\mathcal{S}^3$ .

To apply Gaussian distribution calculations accurately to unit quaternions, we need to consider their geometric properties. We can take advantage of the fact that  $\mathcal{S}^3$  is a Riemannian manifold, map our data to the tangent space at  $(1, [0, 0, 0]^T)$  the Lie algebra ( $\mathbf{L}$ ), apply our calculations there, then finally map the result back to the hypersphere  $\mathcal{S}^3$ . The purpose is to maximize the expected reward as defined in equation (7).

In this sense, let  $\mathcal{M} \equiv \mathcal{S}^3$ ,  $\mathbf{Q} = (v, \mathbf{u})$ ,  $\mathbf{Q}_1 = (v_1, \mathbf{u}_1)$ , and  $\mathbf{Q}_2 = (v_2, \mathbf{u}_2) \in \mathcal{S}^3$ . The logarithmic map,  $\text{Log}_{\mathbf{X}}(\cdot)$  in equations (3)–(7), is then redefined to map  $\mathbf{Q}$  to the Lie algebra, e.g.,  $\text{Log}_{\mathbf{L}}(\cdot) : \mathcal{S}^3 \mapsto \mathcal{R}^3$  [41] as

$$\text{Log}_{\mathbf{L}}(\mathbf{Q}) = \begin{cases} \arccos(v) \frac{\mathbf{u}}{\|\mathbf{u}\|}, & \|\mathbf{u}\| \neq 0 \\ [0, 0, 0]^T, & \|\mathbf{u}\| = 0 \end{cases}, \quad (8)$$

where  $\|\cdot\|$  defines the norm of a vector. This mapping is also used to define a distance metric upon  $\mathcal{S}^3$  [41]

$$\begin{aligned}d(\mathbf{Q}_1, \mathbf{Q}_2) &= \\ \begin{cases} 2\pi, & \mathbf{Q}_1 * \overline{\mathbf{Q}_2} = (-1, [0, 0, 0]^T) \\ 2\|\text{Log}(\mathbf{Q}_1 * \overline{\mathbf{Q}_2})\|, & \text{otherwise} \end{cases},\end{aligned}\quad (9)$$



where  $\bar{\mathbf{Q}}_2 = (v_2, -\mathbf{u}_2)$  is the quaternion conjugate of  $\mathbf{Q}_2$ . The  $*$  denotes the quaternion multiplication which is calculated as follows

$$\mathbf{Q}_1 * \mathbf{Q}_2 = (v_1 v_2 - \mathbf{u}_1 \cdot \mathbf{u}_2, v_1 \mathbf{u}_2 + v_2 \mathbf{u}_1 + \mathbf{u}_1 \times \mathbf{u}_2). \quad (10)$$

For example, if the reward function is  $\exp(-d)$ , where  $d$  is the distance between two unit quaternions, then equation (9) is used to calculate the distance on the tangent space.

The exponential map,  $\text{Exp}_{\mathbf{X}}(\cdot)$  in (6), is redefined to project the learned action  $\mathbf{q}$  from the policy  $\pi_{\theta}$  to the hypersphere  $\mathcal{S}^3$ , e.g.,  $\text{Exp}_{\mathbf{L}}(\cdot) : \mathcal{R}^3 \mapsto \mathcal{S}^3$  [41]

$$\text{Exp}_{\mathbf{L}}(\mathbf{q}) = \begin{cases} \left( \cos(\|\mathbf{q}\|), \sin(\|\mathbf{q}\|) \frac{\mathbf{q}}{\|\mathbf{q}\|} \right), & \|\mathbf{q}\| \neq 0 \\ (1, [0, 0, 0]^{\top}), & \|\mathbf{q}\| = 0 \end{cases}. \quad (11)$$

Our proposed framework, as depicted in Fig.1, is based on having the results of the policy parameterization on the tangent space as in (5), which should be in  $\mathcal{R}^3$ . It is important to ensure the tangent space is bounded as shown in Fig. 2 (b); the open ball with radius  $\pi$  (in other words  $\|\mathbf{q}\| < \pi$ ), and the manifold limited to  $\mathcal{S}^3/(-1, [0, 0, 0]^{\top})$ . This guarantees that the exponential map and the logarithmic map are both one-to-one, continuously differentiable and maintain their inverse relationship to each other as shown in [42]. To respect this limitation of the tangent space, as we perform parameterization we can reject the results whenever it is out of the defined space; e.g., the norm of the sampled vector  $\|\mathbf{q}\| \geq \pi$ . This method of rejection is prone to substantial slowdowns in computational speed, especially when the mean of the distribution is close to the boundary of the open ball in  $\mathcal{R}^3$ .

As a solution that assures the results of parameterization always remain within the boundaries, we propose to parameterize the vector  $\mathbf{q} \in \mathcal{R}^3$  by four parameters. Three of the four parameters are used to learn the direction of  $\mathbf{q}$  by normalizing the  $\mathcal{R}^3$  vector into a unit vector, with its domain between -1 and 1. The final parameter with its domain  $[0, \pi)$  is used as the norm of  $\mathbf{q}$ . The next step is to map the vector  $\mathbf{q}$  to the hypersphere  $\mathcal{S}^3$  using the exponential map (11), where it resolves to a unit quaternion that is passed to the controller of a robot to change the orientation of its end-effector.

## V. EXPERIMENTAL RESULTS

Experiments have been carried out in simulated environments (Wahba [43] and trajectory learning problems), as well as a real setup involving a physical robot performing the Ball-in-a-hole task. Several RL and policy improvement algorithms have been tested:

- deep RL algorithms like SAC [21] and PPO [22],
- the expectation-maximization inspired PoWER algorithm [16], and
- the BBO-based CMA-ES algorithm [12].

Our research question is about the gains of considering the geometry of non-Euclidean data (e.g., orientation) in RL algorithms based on Gaussian distributions, and how they compare with solutions based on other distributions like Bingham.

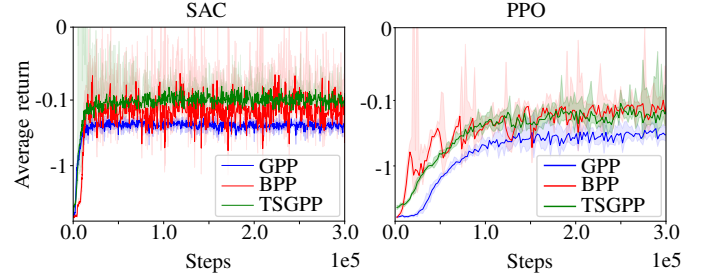


Fig. 3. Wahba domain results for SAC and PPO using GPP, TSGPP, and BPP. The mean (solid lines) and the standard deviation (shaded regions) are calculated over 5 different seeds.

### A. simulation experiments

1) *Wahba problem*: The Wahba problem, first proposed by Grace Wahba in 1965 [43], is about finding the best rotation between two Euclidean coordinate systems that aligns two sets of noisy 3-dimensional vector observations. The original motivation for this problem was in estimating satellite altitudes using vectors from different frames of reference but was later applied to other fields of research as well.

The cost function defines attempts to minimize the difference between sets of vectors ( $\mathbf{y}_i \in Y, \mathbf{z}_i \in Z$ ) by finding a rotation  $\mathbf{R} \in \mathcal{SO}(3)$

$$J(\mathbf{R}) = \frac{1}{2} \sum_{k=1}^N a_k \|\mathbf{z}_k - \mathbf{R} \mathbf{y}_k\|^2. \quad (12)$$

where  $a_k$  are the weights for each observation. In our case, orientation is represented by unit quaternions.

Figure 3 shows the results of learning the orientation represented as a unit quaternion using Gaussian Policy Parameterization (GPP), Tangent Space Gaussian Policy Parameterization (TSGPP), and Bingham Policy Parameterization (BPP) [34]. The quality of the learned policy using TSGPP was better than GPP for both SAC [21] and PPO [22], while compared to BPP a slightly better policy was learned for SAC and a comparable policy was learned for PPO.

We also used a variation of the Wahba problem using PoWER and CMA-ES with 10 observations. As shown in Fig. 4 and Fig. 5, our goal from these experiments is to show the importance of avoiding approximation (normalization) when learning unit quaternions. The results of TSGPP are significantly better than the GPP results.

2) *Orientation Trajectory learning problem*: Some manipulation learning problems require learning a desired trajectory of the end-effector pose. In this section, we focus on learning a trajectory of orientations where a policy is trained to follow a well-defined trajectory. In this problem, we used the PoWER and CMA-ES algorithms to learn trajectories with different lengths as shown in Fig. 6 and Fig. 7. We observe that the TSGPP results are significantly better than the GPP results.

### B. real experiments (Ball-in-a-hole)

The Ball-in-a-hole problem is a new benchmark proposed in this paper inspired by the Ball-in-a-cup [44] and the ball balancing [45] problems. The problem setup is as depicted in

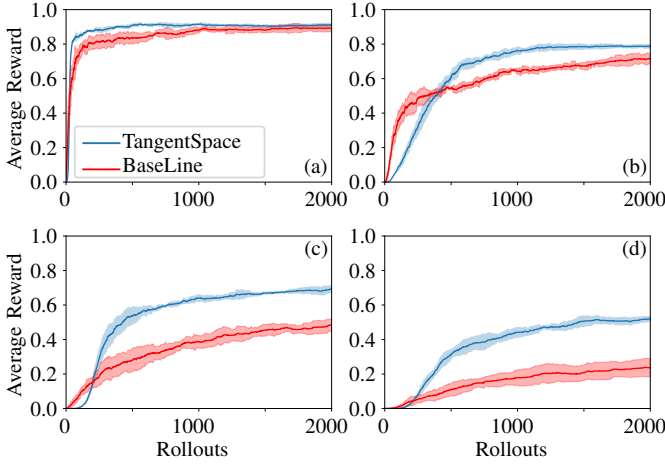


Fig. 4. Four instances of a variation of the Wahba problem with different sizes (complexity) solved by the PoWER algorithm. Size for each is (a) 3, (b) 5, (c) 7, and (d) 9. The mean (solid lines) and the standard deviation (shaded regions) are calculated over 5 different seeds.

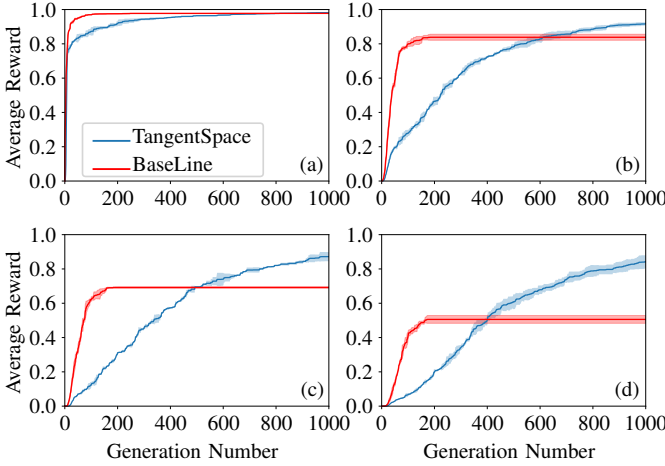


Fig. 5. Four instances of a variation of the Wahba problem with different sizes (complexity) solved by the CMA-ES algorithm. Size for each is (a) 3, (b) 5, (c) 7, and (d) 9. The mean (solid lines) and the standard deviation (shaded regions) are calculated over 5 different seeds.

Fig. 8, where a plate with a hole in the middle is attached to the end-effector of the TM5-900 Collaborative Robot (cobot). A camera is also attached to the end effector of the robot and is on a stand to always face the surface of the plate. A ping-pong ball is present on the plate, which has its position tracked by the camera. The robot's end-effector position is fixed with only its orientation being changed, and the reward is represented by  $\exp^{-d}$ , where  $d$  is the distance between the center of the ball and the center of the hole measured using the vision system. As this is a challenging problem (lightweight ball, noise in the vision system, and with position control), we decided to start each rollout with the ball in the same initial position.

Regarding the limitations of the TM5-900 cobot, real-time communication is not guaranteed as all communications pass through the TM-Flow software using a Position, Velocity, Time (PVT) function. No variable impedance control or admittance control is possible as of writing this paper. Therefore,

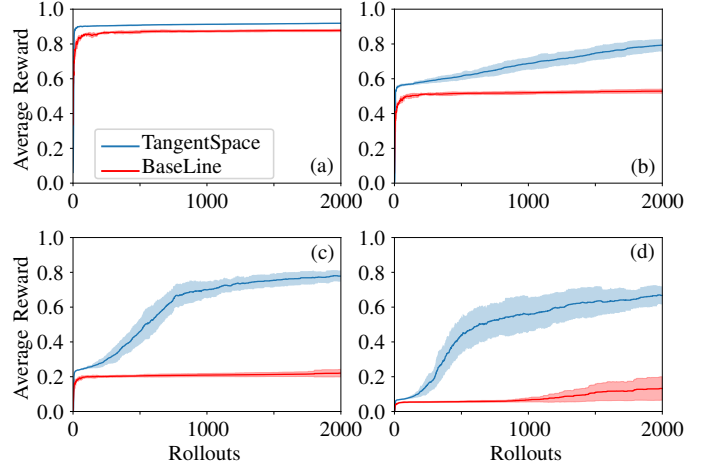


Fig. 6. Four instances of the orientation trajectory learning problem with different lengths (complexity) solved by the PoWER algorithm. Length for each is (a) 5, (b) 10, (c) 15, and (d) 20. The mean (solid lines) and the standard deviation (shaded regions) are calculated over 5 different seeds.

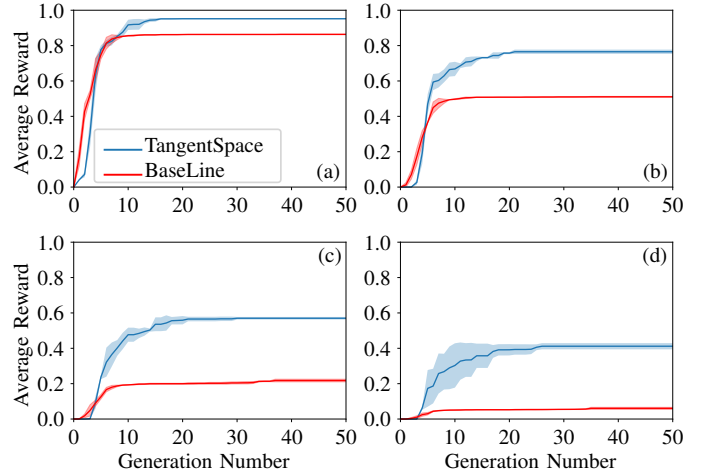


Fig. 7. Four instances of the orientation trajectory learning problem with different lengths (complexity) solved by the CMA-ES algorithm. Length for each is (a) 5, (b) 10, (c) 15, and (d) 20. The mean (solid lines) and the standard deviation (shaded regions) are calculated over 5 different seeds.

we had to split the trajectory from one rollout into a number of steps. After each orientation change, the ball's location was immediately read and included in the terminal reward (used to guide the RL algorithm). We used the PoWER algorithm to learn a policy that moves the ball into the hole, with Fig. 9 showing the results of the experiment. The algorithm eventually converged to a local policy, where it learned how to place the ball in the hole via a single axis as seen in the demonstration video.

## VI. DISCUSSION

As noted in the experimental results (Sec. V-A), for simple problems the baseline GPP may converge faster than TSGPP at the same quality solution. An example is shown in Fig. 5(a). As the effect of normalization is negligible in these cases, the benefit of utilizing the tangent space projection is limited. However, analyzing the results in more complex problems, it is possible to observe that, while TSGPP takes longer to converge

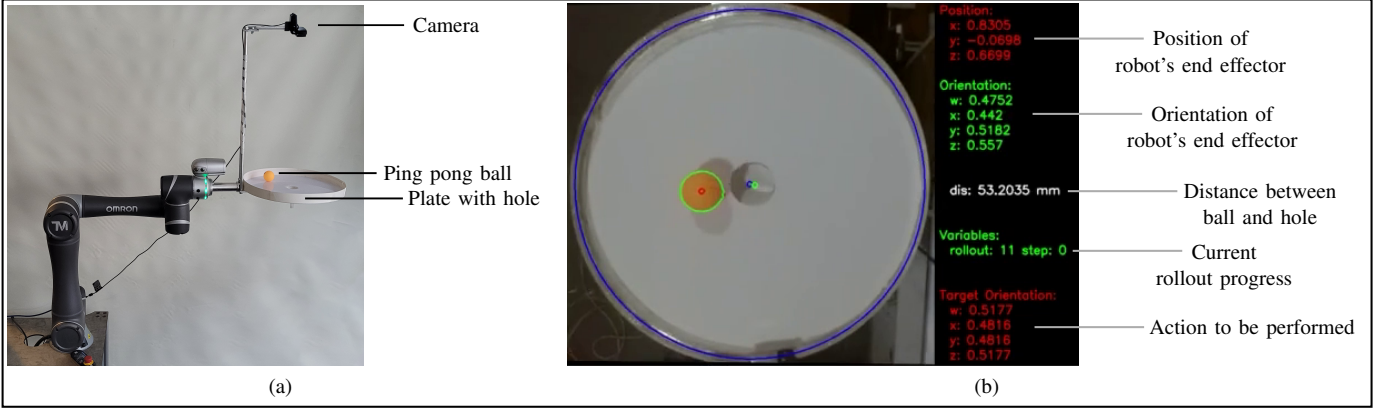


Fig. 8. (a) Ball-in-a-hole problem setup. A plate with a hole in the middle is attached to the end-effector of the robot. The circumference of the plate is surrounded by cardboard so that the ball does not fall outside the plate. A ping pong ball is located on the top of the plate. A camera is also attached to the end-effector in order to measure the distance between the center of the ball and the center of the hole. (b) shows the plate view using the top camera, and the data captured from both the vision system and the robot controller.

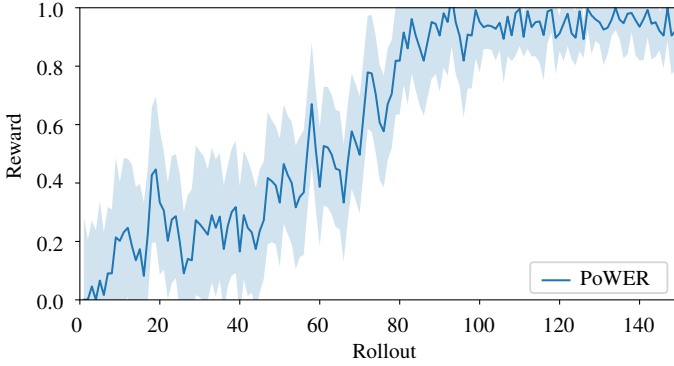


Fig. 9. The expected return of the learned policy in the Ball-in-a-hole evaluation, averaged over 5 runs.

than GPP, TSGPP ultimately reaches a better quality solution (see, for instance, Fig. 7(a)). This allows us to conclude that in moderately complex problems, the error caused by normalization is significant enough to affect the quality of the solution and there is a clear advantage in using the proposed TSGPP.

As already noted in [34], BPP parameterization relies on the prediction from multiple neural networks and this may introduce significant approximation errors. Unlike GPP and TSGPP, this culminates in an unstable learning process. We have experimentally observed this problem of BPP and several attempts were made before representative results were achieved with this approach. On the contrary, the stability of TSGPP was on par with GPP, and better than BPP, verifying that the one-to-one mappings between the manifold and tangent space are stable.

We experimentally observed that the average computational overhead of TSGPP over GPP is about 3% for SAC and 6% for PPO. These results were expected as the mappings between the tangent space and manifold are not computationally expensive, and it is straightforward to implement. This contrasts with BPP, for which we have observed an average overhead of about 33% for SAC and 118% for PPO. Moreover, BPP involves modifying the distribution and customizing the algo-

rithm to fit. Therefore, we conclude that TSGPP can provide a noticeable improvement in solution quality over GPP at the cost of a small performance penalty and that it can deliver at least equal results to BPP while performing much faster.

Despite the improvement in accuracy, parameterizing in tangent space is most beneficial where data points are in the neighborhood of the origin of the tangent space. This is due to the tangent space projection that locally preserves distances near the origin, while distances measured away from the origin are less accurate. This is a limitation of applying policy parameterization on tangent space and we expect it can significantly affect the performance in settings where the policy is integrated over time (e.g., to generate orientations from a velocity command). However, this case was not studied in this work and, in the considered problems, TSGPP always results in accurate learning.

## VII. CONCLUSION

Applying RL algorithms on geometric data like orientation or stiffness is common in robotics, and these algorithms usually perform better when considering the unique structure of these data. The current study was generally dedicated to this topic, and showed how RL can be applied to learn orientation (as a case study) in the task space (represented by unit quaternions); parameterization and optimization are carried on the tangent space, and the policy evaluation is carried on the hypersphere  $S^3$ . We found that adapting the Gaussian distribution, which is simple and powerful, to the geometry of non-Euclidean data makes it competitive with alternative distributions (e.g., Bingham). Empirical results on both simulation and the physical robot reflect the importance of considering the geometry of non-Euclidean data, and how the performance and accuracy of the overall learning process are consequently affected.

## REFERENCES

- [1] L. Kunze, N. Hawes, T. Duckett, M. Hanheide, and T. Krajník, "Artificial intelligence for long-term robot autonomy: A survey," *IEEE Robotics and Automation Letters*, vol. 3, no. 4, pp. 4023–4030, 2018.

- [2] S. Padakandla, "A survey of reinforcement learning algorithms for dynamically varying environments," *ACM Computing Surveys (CSUR)*, vol. 54, no. 6, pp. 1–25, 2021.
- [3] M. Naeem, S. T. H. Rizvi, and A. Coronato, "A gentle introduction to reinforcement learning and its application in different fields," *IEEE Access*, vol. 8, pp. 209 320–209 344, 2020.
- [4] K. Arulkumaran, M. P. Deisenroth, M. Brundage, and A. A. Bharath, "A brief survey of deep reinforcement learning," *arXiv preprint arXiv:1708.05866*, 2017.
- [5] K. Chatzilygeroudis, V. Vassiliades, F. Stulp, S. Calinon, and J.-B. Mouret, "A survey on policy search algorithms for learning robot controllers in a handful of trials," *IEEE Transactions on Robotics*, vol. 36, no. 2, pp. 328–347, 2019.
- [6] J. Kober, J. A. Bagnell, and J. Peters, "Reinforcement learning in robotics: A survey," *The International Journal of Robotics Research*, vol. 32, no. 11, pp. 1238–1274, 2013.
- [7] S. Ambhore, "A comprehensive study on robot learning from demonstration," in *2020 2nd International Conference on Innovative Mechanisms for Industry Applications (ICIMIA)*. IEEE, 2020, pp. 291–299.
- [8] S. Arora and P. Doshi, "A survey of inverse reinforcement learning: Challenges, methods and progress," *Artificial Intelligence*, vol. 297, p. 103500, 2021.
- [9] B. Piot, M. Geist, and O. Pietquin, "Bridging the gap between imitation learning and inverse reinforcement learning," *IEEE transactions on neural networks and learning systems*, vol. 28, no. 8, pp. 1814–1826, 2016.
- [10] Y. Ge, F. Zhu, X. Ling, and Q. Liu, "Safe q-learning method based on constrained markov decision processes," *IEEE Access*, vol. 7, pp. 165 007–165 017, 2019.
- [11] F. Stulp and O. Sigaud, "Policy improvement: Between black-box optimization and episodic reinforcement learning," in *Journées Francophones Planification, Décision, et Apprentissage pour la conduite de systèmes*, 2013.
- [12] N. Hansen, "The cma evolution strategy: a comparing review," *Towards a new evolutionary computation*, pp. 75–102, 2006.
- [13] M. J. Zeestraten, "Programming by demonstration on riemannian manifolds." Ph.D. dissertation, University of Genoa, Italy, 2018.
- [14] X. Pennec, "Intrinsic statistics on riemannian manifolds: Basic tools for geometric measurements," *Journal of Mathematical Imaging and Vision*, vol. 25, no. 1, pp. 127–154, 2006.
- [15] E. Theodorou, J. Buchli, and S. Schaal, "A generalized path integral control approach to reinforcement learning," *The Journal of Machine Learning Research*, vol. 11, pp. 3137–3181, 2010.
- [16] J. Kober and J. Peters, "Policy search for motor primitives in robotics," *Machine learning*, vol. 84, no. 1, pp. 171–203, 2011.
- [17] K. Chatzilygeroudis, R. Rama, R. Kaushik, D. Goepf, V. Vassiliades, and J.-B. Mouret, "Black-box data-efficient policy search for robotics," in *2017 IEEE/RSJ International Conference on Intelligent Robots and Systems (IROS)*. IEEE, 2017, pp. 51–58.
- [18] M. Saveriano, Y. Yin, P. Falco, and D. Lee, "Data-efficient control policy search using residual dynamics learning," in *IEEE/RSJ International Conference on Intelligent Robots and Systems*, 2017, pp. 4709–4715.
- [19] T. P. Lillicrap, J. J. Hunt, A. Pritzel, N. Heess, T. Erez, Y. Tassa, D. Silver, and D. Wierstra, "Continuous control with deep reinforcement learning," *arXiv preprint arXiv:1509.02971*, 2015.
- [20] S. Fujimoto, H. Hoof, and D. Meger, "Addressing function approximation error in actor-critic methods," in *International conference on machine learning*. PMLR, 2018, pp. 1587–1596.
- [21] T. Haarnoja, A. Zhou, K. Hartikainen, G. Tucker, S. Ha, J. Tan, V. Kumar, H. Zhu, A. Gupta, P. Abbeel *et al.*, "Soft actor-critic algorithms and applications," *arXiv preprint arXiv:1812.05905*, 2018.
- [22] J. Schulman, F. Wolski, P. Dhariwal, A. Radford, and O. Klimov, "Proximal policy optimization algorithms," *arXiv preprint arXiv:1707.06347*, 2017.
- [23] F. J. Abu-Dakka, Y. Huang, J. Silvério, and V. Kyrki, "A probabilistic framework for learning geometry-based robot manipulation skills," *Robotics and Autonomous Systems*, vol. 141, p. 103761, 2021.
- [24] M. J. Zeestraten, I. Havoutis, J. Silvério, S. Calinon, and D. G. Caldwell, "An approach for imitation learning on riemannian manifolds," *IEEE Robotics and Automation Letters*, vol. 2, no. 3, pp. 1240–1247, 2017.
- [25] M. J. Zeestraten, I. Havoutis, S. Calinon, and D. G. Caldwell, "Learning task-space synergies using riemannian geometry," in *2017 IEEE/RSJ International Conference on Intelligent Robots and Systems (IROS)*. IEEE, 2017, pp. 73–78.
- [26] B. Ti, Y. Gao, J. Zhao, and S. Calinon, "Imitation of manipulation skills using multiple geometries," *arXiv preprint arXiv:2203.01171*, 2022.
- [27] L. Rozo and V. Dave, "Orientation probabilistic movement primitives on riemannian manifolds," in *Conference on Robot Learning*. PMLR, 2022, pp. 373–383.
- [28] Y. Huang, F. J. Abu-Dakka, J. Silvério, and D. G. Caldwell, "Toward orientation learning and adaptation in cartesian space," *IEEE Transactions on Robotics*, vol. 37, no. 1, pp. 82–98, 2020.
- [29] H. Beik-Mohammadi, S. Hauberg, G. Arvanitidis, G. Neumann, and L. Rozo, "Learning riemannian manifolds for geodesic motion skills," *arXiv preprint arXiv:2106.04315*, 2021.
- [30] S. Colutto, F. Fruhauf, M. Fuchs, and O. Scherzer, "The cma-es on riemannian manifolds to reconstruct shapes in 3-d voxel images," *IEEE Transactions on Evolutionary Computation*, vol. 14, no. 2, pp. 227–245, 2009.
- [31] J. Chen, Y. Yin, T. Birdal, B. Chen, L. J. Guibas, and H. Wang, "Projective manifold gradient layer for deep rotation regression," in *Proceedings of the IEEE/CVF Conference on Computer Vision and Pattern Recognition*, 2022, pp. 6646–6655.
- [32] N. Jaquier, L. Rozo, S. Calinon, and M. Bürger, "Bayesian optimization meets riemannian manifolds in robot learning," in *Conference on Robot Learning*. PMLR, 2020, pp. 233–246.
- [33] N. Jaquier, V. Borovitskiy, A. Smolensky, A. Terenin, T. Asfour, and L. Rozo, "Geometry-aware bayesian optimization in robotics using riemannian matern kernels," in *Conference on Robot Learning*. PMLR, 2022, pp. 794–805.
- [34] S. James and P. Abbeel, "Bingham policy parameterization for 3d rotations in reinforcement learning," *arXiv preprint arXiv:2202.03957*, 2022.
- [35] R. S. Sutton and A. G. Barto, *Reinforcement learning: An introduction*. MIT press, 2018.
- [36] J. Kober, "Learning motor skills: from algorithms to robot experiments," Ph.D. dissertation, Technische Universität, 2012.
- [37] M. M. Bronstein, J. Bruna, Y. LeCun, A. Szlam, and P. Vandergheynst, "Geometric deep learning: going beyond euclidean data," *IEEE Signal Processing Magazine*, vol. 34, no. 4, pp. 18–42, 2017.
- [38] S. Calinon, "Gaussians on Riemannian manifolds: Applications for robot learning and adaptive control," *IEEE Robotics and Automation Magazine (RAM)*, vol. 27, no. 2, pp. 33–45, June 2020.
- [39] F. J. Abu-Dakka and V. Kyrki, "Geometry-aware dynamic movement primitives," in *2020 IEEE International Conference on Robotics and Automation (ICRA)*. IEEE, 2020, pp. 4421–4426.
- [40] R. M. Murray, Z. Li, and S. S. Sastry, *A mathematical introduction to robotic manipulation*. CRC press, 2017.
- [41] A. Ude, "Filtering in a unit quaternion space for model-based object tracking," *Robotics and Autonomous Systems*, vol. 28, no. 2-3, pp. 163–172, 1999.
- [42] A. Ude, B. Nemec, T. Petrić, and J. Morimoto, "Orientation in cartesian space dynamic movement primitives," in *2014 IEEE International Conference on Robotics and Automation (ICRA)*. IEEE, 2014, pp. 2997–3004.
- [43] G. Wahba, "A least squares estimate of satellite attitude," *SIAM review*, vol. 7, no. 3, pp. 409–409, 1965.
- [44] C. Sumners, "Toys in space: Exploring science with the astronauts," 1994.
- [45] M. M. Kopichev, A. V. Putov, and A. N. Pashenko, "Ball on the plate balancing control system," in *IOP Conference Series: Materials Science and Engineering*, vol. 638, no. 1. IOP Publishing, 2019, p. 012004.



**NASEEM ALHOUSANI** received his B.Sc. in computer science and M.Sc. in scientific computing from Birzeit University in 2003 and 2006 respectively. He is currently pursuing a Ph.D. degree in computer engineering at Istanbul Technical University, Istanbul, Turkey. From 2006 to 2015 he worked as a lecturer in the computer science department at Palestine Technical University – Kadoorie. Since 2015 he is a Researcher at ILITRON energy and technology, Istanbul, Turkey. His research interest includes reinforcement learning, planning, and learning on Riemannian manifolds.



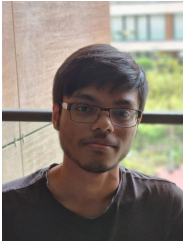
**Matteo Saveriano** received his B.Sc. and M.Sc. degree in automatic control engineering from University of Naples, Italy, in 2008 and 2011, respectively. He received his Ph.D. from the Technical University of Munich in 2017. Currently, he is an assistant professor at the Department of Industrial Engineering (DII), University of Trento, Italy. Previously, he was an assistant professor at the University of Innsbruck and a post-doctoral researcher at the German Aerospace Center (DLR). He is an Associate Editor for RA-L. His research activities include robot learning, human-robot interaction, understanding and interpreting human activities. Webpage: <https://matteosaveriano.weebly.com/>



**Fares J. Abu-Dakka** received his B.Sc. degree in mechanical engineering from Birzeit University, Palestine, in 2003, and his M.Sc. and Ph.D. degrees in robotics motion planning from the Polytechnic University of Valencia, Spain, in 2006 and 2011, respectively. Currently, he is a senior researcher at Intelligent Robotics Group at EEA, Aalto University, Finland. Previously, he was researching at ADVR, Istituto Italiano di Tecnologia (IIT). Between 2013 and 2016 he was holding a visiting professor position at ISA of the Carlos III University of Madrid, Spain. He is an Associate Editor for ICRA, IROS, and RA-L. His research activities include robot learning & control, and human-robot interaction. Webpage: <https://sites.google.com/view/abudakka/>



**IBRAHIM SEVINC** continues his B.Sc. degree in Electronics and Communication Engineering at Istanbul Technical University, Turkey. He has been working at ILITRON Energy and Information Technologies, Istanbul, Turkey since 2020.



**TALHA ABDULKUDDUS** is working towards his B.Sc. Computer Science degree at King's College London, UK. Since 2022, he started working at ILITRON Energy and Information Technologies, Istanbul, Turkey.



**Hatice Kose** is a full Professor at Faculty of Computer and Informatics Engineering, Istanbul Technical University, Turkey, coordinating the GameLab and Cognitive Social Robotics Lab, since 2010. She received her Ph.D. degree from the Computer Engineering Department, Bogazici University, Turkey. From 2006-2010, she worked as a Research Fellow at the University of Hertfordshire. Her current research focuses on gesture communication (involving sign language) and imitation-based interaction games with social humanoid robots for the education and rehabilitation of children with hearing impairment and children with ASD. She is leading several national projects and taking part in several Horizon2020 projects, Erasmus+ and Cost actions, on social assistive robots, sign language tutoring robots, and human-robot interaction.